

Electron transport in magnetic multilayers: Effect of disorder

V. Drchal,^{1,2} J. Kudrnovský,^{1,2,4} P. Bruno,⁴ P. H. Dederichs,⁵ I. Turek,^{2,3,6} and P. Weinberger²

¹*Institute of Physics, Academy of Sciences of the Czech Republic, Na Slovance 2, CZ-182 21 Prague 8, Czech Republic*

²*Center for Computational Materials Science, Technical University of Vienna, Getreidemarkt 9/158, A-1060 Vienna, Austria*

³*Institute of Physics of Materials, Academy of Sciences of the Czech Republic, Žitkova 22, CZ-616 62 Brno, Czech Republic*

⁴*Max-Planck-Institut für Mikrostrukturphysik, Weinberg 2, D-06120 Halle, Germany*

⁵*Institut für Festkörperforschung, Forschungszentrum Jülich, D-52425 Jülich, Germany*

⁶*Department of Electronic Structures, Charles University, Ke Karlovu 5, 121 16 Praha 2, Czech Republic*

(Received 22 October 2001; revised manuscript received 22 March 2002; published 29 May 2002)

The magnetoresistance of metallic multilayers in the current-perpendicular-to-plane (CPP) geometry is studied theoretically on an *ab initio* level using the tight-binding linear muffin-tin orbital method. The applied potential parameters were determined self-consistently for a given alloy composition within the coherent potential approximation (CPA). Lateral supercells with random arrangements of atoms of two types are used to represent disorder connected with interface interdiffusion and with alloying in the spacer. We distinguish ballistic and diffusive parts of transport and study their dependence on the type and on the strength of disorder. The theoretical approach is illustrated on disordered systems derived from the fcc-based Co|Cu|Co(001) trilayers that serve as the reference system. We find quite a good agreement with experimental data and with other calculations. On the other hand, our results also show the limited validity of the two-current series-resistor model and that vertex corrections to the CPA applied to the CPP transport are of great importance.

DOI: 10.1103/PhysRevB.65.214414

PACS number(s): 75.70.Pa, 72.10.Fk

I. INTRODUCTION

The giant magnetoresistance (GMR) in metallic magnetic multilayers is said to be due to spin-dependent scattering.^{1,2} Two types of scattering occur, namely, (i) scattering at the interfaces between different slabs (intrinsic defects), leading to ballistic transport, and (ii) scattering at impurities, substitutional disorder or irregularities of interfaces (extrinsic defects) leading to diffusive transport. In real multilayers both types play a role, and also dislocations and stacking faults can occur. In addition, magnons and phonons can cause dynamical perturbations.

In the diffusive regime the mean free path is much shorter than the dimension of the active part of the multilayer system, i.e., the whole system with exception of the leads. On the other hand, in the ballistic regime the mean free path is larger than the active part of the multilayer system.

The aim of this paper is to study on an *ab initio* level the effect of disorder onto current-perpendicular-to-plane (CPP) transport in magnetic multilayers and investigate the crossover from ballistic to diffusive regime with increasing disorder. In our approach the electronic structure of the system is determined within the tight-binding linear muffin-tin orbital (TB-LMTO) method³ and the conductances are calculated in terms of a Landauer-type formula of linear response theory⁴ formulated in terms of surface Green functions. The randomness is approximately represented by lateral two-dimensional supercells with random occupation of lattice sites by two kinds of atoms. The applications discussed refer to Co|Cu|Co(001)-based trilayers connected to ideal semi-infinite Cu leads. We also reexamine the validity of the two-current series-resistor model and show that it is justified only in the limit of diffusive transport.

II. THEORY

A. Description of the system

Suppose the magnetic multilayer system consists of non-random semi-infinite left and right leads sandwiching a trilayer consisting of a left and a right magnetic slab separated by a nonmagnetic spacer of varying thickness. The left and right leads and magnetic slabs can consist of different metals. A special case of a trilayer consists of nonrandom semi-infinite left and right magnetic leads sandwiching a nonmagnetic spacer.

Multilayers with substitutional disorder in the active region can be represented by finite two-dimensional supercells, each containing several lattice sites occupied randomly by atoms of two (or more) different types. The stacking of random supercells in the growth direction can be arbitrary. These supercells are repeated periodically within planes of atoms. In order to describe disorder (substitutional alloys) it is then necessary to average over different occupations of the sites within a given supercell by the constituents involved and, at the end, to check the dependence of conductances on the supercell size. Quite clearly, such an approach applies to disordered spacers and/or magnetic slabs as well as to disordered interfaces.

B. Electronic structure

The electronic structure of the system is described in terms of the TB-LMTO method. We assume a collinear spin structure and that spin σ is a good quantum number, neglect relativistic effects as well as possible layer and lattice relaxations. The details can be found in Ref. 4.

Consider a parent lattice⁵ with one atom at \mathbf{t}_0 in the two-dimensional elementary cell with translation vectors \mathbf{a}_1 and \mathbf{a}_2 . The corresponding basis vectors of the two-dimensional

reciprocal space are \mathbf{b}_1 and \mathbf{b}_2 . Let us assume that the supercell translation vectors are $\mathbf{A}_1 = M_1 \mathbf{a}_1$ and $\mathbf{A}_2 = M_2 \mathbf{a}_2$. The basis vectors of the supercell reciprocal space are $\mathbf{B}_1 = \mathbf{b}_1 / M_1$ and $\mathbf{B}_2 = \mathbf{b}_2 / M_2$. The supercell contains $M = M_1 M_2$ atoms located at $\mathbf{t}_n = n_1 \mathbf{a}_1 + n_2 \mathbf{a}_2 + \mathbf{t}_0$. Here we use the compound index $n = (n_1, n_2)$, $0 \leq n_i \leq M_i - 1$. The reciprocal lattice vectors $\mathbf{Q}_j = j_1 \mathbf{B}_1 + j_2 \mathbf{B}_2$, where $j = (j_1, j_2)$, map the supercell surface Brillouin zone (SCSBZ) onto the original surface Brillouin zone (SBZ) such that for each $\mathbf{k}_\parallel \in \text{SBZ}$ there exists just one $\mathbf{q}_\parallel \in \text{SCSBZ}$ and just one \mathbf{Q}_j ($0 \leq j_i \leq M_i - 1$) so that $\mathbf{k}_\parallel = \mathbf{q}_\parallel + \mathbf{Q}_j$.

The basis states in the case of an elementary cell with a single atom are

$$|\mathbf{k}_\parallel L \sigma\rangle = \frac{1}{\sqrt{N_\parallel}} \sum_{\mathbf{R}} \exp(i\mathbf{k}_\parallel \cdot \mathbf{R}) |\mathbf{R} L \sigma\rangle, \quad (1)$$

where N_\parallel is the number of lattice sites in the basic region of the atomic plane, summation runs over all lattice sites \mathbf{R} of the plane, $L = (lm)$ is the orbital index, and σ denotes the z projection of the spin. In the supercell case,

$$|n\mathbf{q}_\parallel L \sigma\rangle = \frac{1}{\sqrt{N_\parallel^{\text{SC}}}} \sum_{\mathbf{R} \in S_n} \exp(i\mathbf{q}_\parallel \cdot \mathbf{R}) |\mathbf{R} L \sigma\rangle, \quad (2)$$

where $N_\parallel^{\text{SC}} = N_\parallel / M$ is the number of supercells in the basic region of the atomic plane, S_n denotes the subset of all the lattice sites in the plane such that $\mathbf{R} = m_1 \mathbf{A}_1 + m_2 \mathbf{A}_2 + \mathbf{t}_n$, where m_1 and m_2 are arbitrary integers. The mutual relations between these two bases are

$$|\mathbf{k}_\parallel L \sigma\rangle = \frac{1}{\sqrt{M}} \sum_{n=1}^M \exp(i\mathbf{Q}_j \cdot \mathbf{t}_n) |n\mathbf{q}_\parallel L \sigma\rangle, \quad (3)$$

$$|n\mathbf{q}_\parallel L \sigma\rangle = \frac{1}{\sqrt{M}} \sum_{j=1}^M \exp(-i\mathbf{Q}_j \cdot \mathbf{t}_n) |\mathbf{k}_\parallel L \sigma\rangle, \quad (4)$$

where the vectors \mathbf{k}_\parallel , \mathbf{q}_\parallel , and \mathbf{Q}_j satisfy the condition $\mathbf{k}_\parallel = \mathbf{q}_\parallel + \mathbf{Q}_j$.

C. Transport properties

The conductance per one supercell, i.e., per M interface atoms, can be expressed as⁴

$$C_A = \sum_{\sigma} C_A^{\sigma}, \quad C_A^{\sigma} = \frac{e^2}{h} \frac{1}{N_\parallel^{\text{SC}}} \sum_{\mathbf{q}_\parallel} \sum_{nL} T_{nL,nL}^{A,\sigma}(\mathbf{q}_\parallel, E_F), \quad (5)$$

where E_F is the Fermi energy, e is the electron charge, h is the Planck's constant (the quantity e^2/h is usually called the conductance quantum), and $A = \text{P}$ (AP) denotes the parallel (antiparallel) orientation of magnetizations of the magnetic slabs. The transmittance $T_{nL,n'L'}^{\sigma}(\mathbf{q}_\parallel, E)$ is given by

$$\begin{aligned} T_{nL,n'L'}^{\sigma}(\mathbf{q}_\parallel, E) = & \lim_{\delta \rightarrow 0+} \frac{1}{2} \{ B_1^{\beta,\sigma}(\mathbf{q}_\parallel, E) g_{1,N}^{\beta,\sigma}(\mathbf{q}_\parallel, z_+) \\ & \times B_N^{\beta,\sigma}(\mathbf{q}_\parallel, E) g_{N,1}^{\beta,\sigma}(\mathbf{q}_\parallel, z_-) \\ & + B_1^{\beta,\sigma}(\mathbf{q}_\parallel, E) g_{1,N}^{\beta,\sigma}(\mathbf{q}_\parallel, z_-) \\ & \times B_N^{\beta,\sigma}(\mathbf{q}_\parallel, E) g_{N,1}^{\beta,\sigma}(\mathbf{q}_\parallel, z_+) \}_{nL,n'L'}, \quad (6) \end{aligned}$$

where $z_{\pm} = E \pm i\delta$. The quantities $B_1^{\sigma}(\mathbf{q}_\parallel, E)$ and $B_N^{\sigma}(\mathbf{q}_\parallel, E)$ are the anti-Hermitian parts of the embedding potentials of the left and right lead, respectively, and $g_{1,N}^{\beta,\sigma}(\mathbf{q}_\parallel, z)$ and $g_{N,1}^{\beta,\sigma}(\mathbf{q}_\parallel, z)$ are blocks of the auxiliary Green function connecting the boundary layers 1 and N of the active region.

The magnetoresistance ratio is defined as

$$R_{\text{CPP}} = \mathcal{R}_{\text{AP}} / \mathcal{R}_{\text{P}} - 1 = C_{\text{P}} / C_{\text{AP}} - 1, \quad (7)$$

where $\mathcal{R}_A = 1/C_A$ is the resistance per interface atom or per one supercell. Partial resistances $\mathcal{R}_A^{\sigma} = 1/C_A^{\sigma}$ are defined in a similar way.

D. Ballistic and diffusive transport

If the parent lattice is randomly occupied by atoms of two types, the electrons are scattered by disorder in the active region. The motion of an electron can be either ballistic (if \mathbf{k}_\parallel is conserved) or diffusive (if \mathbf{k}_\parallel is not conserved). Here, \mathbf{k}_\parallel is a vector from the SBZ of the parent lattice.

The total conductance given by

$$C = \sum_{\sigma} C^{\sigma}, \quad C^{\sigma} = \frac{e^2}{h} \frac{1}{N_\parallel} \sum_{\mathbf{k}_\parallel} \sum_{\mathbf{k}'_\parallel} \sum_L T_{LL}^{\sigma}(\mathbf{k}_\parallel, \mathbf{k}'_\parallel, E_F) \quad (8)$$

can be divided into its ballistic part

$$C_{\text{ball}} = \sum_{\sigma} C_{\text{ball}}^{\sigma}, \quad C_{\text{ball}}^{\sigma} = \frac{e^2}{h} \frac{1}{N_\parallel} \sum_{\mathbf{k}_\parallel} \sum_L T_{LL}^{\sigma}(\mathbf{k}_\parallel, \mathbf{k}_\parallel, E_F), \quad (9)$$

and diffusive part

$$C_{\text{diff}} = \sum_{\sigma} C_{\text{diff}}^{\sigma}, \quad C_{\text{diff}}^{\sigma} = \frac{e^2}{h} \frac{1}{N_\parallel} \sum_{\mathbf{k}_\parallel \neq \mathbf{k}'_\parallel} \sum_L T_{LL}^{\sigma}(\mathbf{k}_\parallel, \mathbf{k}'_\parallel, E_F). \quad (10)$$

The transmittance $T_{LL'}^{\sigma}(\mathbf{k}_\parallel, \mathbf{k}'_\parallel, E)$ is given by

$$\begin{aligned} T_{LL'}^{\sigma}(\mathbf{k}_\parallel, \mathbf{k}'_\parallel, E) = & \frac{1}{2} \lim_{\delta \rightarrow 0+} \{ B_1^{\beta,\sigma}(\mathbf{k}_\parallel, E) g_{1,N}^{\beta,\sigma}(\mathbf{k}_\parallel, \mathbf{k}'_\parallel, z_+) \\ & \times B_N^{\beta,\sigma}(\mathbf{k}'_\parallel, E) g_{N,1}^{\beta,\sigma}(\mathbf{k}'_\parallel, \mathbf{k}_\parallel, z_-) \\ & + B_1^{\beta,\sigma}(\mathbf{k}_\parallel, E) g_{1,N}^{\beta,\sigma}(\mathbf{k}_\parallel, \mathbf{k}'_\parallel, z_-) \\ & \times B_N^{\beta,\sigma}(\mathbf{k}'_\parallel, E) g_{N,1}^{\beta,\sigma}(\mathbf{k}'_\parallel, \mathbf{k}_\parallel, z_+) \}_{LL'}. \quad (11) \end{aligned}$$

The above formulas are valid for systems with one atom at \mathbf{t}_0 in the elementary cell of the parent lattice.

The transport in supercells with a perfect 2D lateral periodicity is ballistic because the \mathbf{q}_{\parallel} vectors from the SCSBZ are conserved. On the other hand, the vectors $\mathbf{k}_{\parallel} = \mathbf{q}_{\parallel} + \mathbf{Q}_j$ from the SBZ are not conserved. As it was first shown in Ref. 6, the results of supercell calculations can be used to separate the ballistic and diffusive parts of the electron motion.

Using Eqs. (3) and (4) it is straightforward to show that

$$T_{LL'}^{\sigma}(\mathbf{k}_{\parallel}, \mathbf{k}'_{\parallel}, E) = \frac{1}{M} \sum_{n=1}^M \sum_{n'=1}^M \exp[-i\mathbf{Q}_j \cdot \mathbf{t}_n + i\mathbf{Q}_{j'} \cdot \mathbf{t}_{n'}] \times T_{nL, n'L'}^{\sigma}(\mathbf{q}_{\parallel}), \quad (12)$$

where $\mathbf{Q}_j = \mathbf{k}_{\parallel} - \mathbf{q}_{\parallel}$ and $\mathbf{Q}_{j'} = \mathbf{k}'_{\parallel} - \mathbf{q}_{\parallel}$.

The conductance can be calculated approximately within the coherent potential approximation (CPA) if the vertex corrections are neglected. The auxiliary Green functions $g_{1,N}^{\beta,\sigma}(\mathbf{k}_{\parallel}, \mathbf{k}'_{\parallel}, z)$ and $g_{N,1}^{\beta,\sigma}(\mathbf{k}'_{\parallel}, \mathbf{k}_{\parallel}, z)$ in Eq. (11) are then replaced by their CPA averages $\delta_{\mathbf{k}_{\parallel}, \mathbf{k}'_{\parallel}} \langle g_{1,N}^{\beta,\sigma}(\mathbf{k}_{\parallel}, z) \rangle_{\text{CPA}}$ and $\delta_{\mathbf{k}_{\parallel}, \mathbf{k}'_{\parallel}} \langle g_{N,1}^{\beta,\sigma}(\mathbf{k}_{\parallel}, z) \rangle_{\text{CPA}}$, respectively. As it will be shown later, the CPA and ballistic conductances are quite similar. The reason is that the CPA one-particle propagators $\langle g_{1,N}^{\beta,\sigma}(\mathbf{k}_{\parallel}, z) \rangle_{\text{CPA}}$ and $\langle g_{N,1}^{\beta,\sigma}(\mathbf{k}_{\parallel}, z) \rangle_{\text{CPA}}$ do not contain scattering from the \mathbf{k}_{\parallel} state to a different \mathbf{k}'_{\parallel} state. Consequently, in this case within the CPA without vertex corrections, the diffusive transport is completely missing. On the other hand, the damping of the ballistic transport is described qualitatively quite well because the imaginary part of the CPA self-energy mimics the particle losses from the \mathbf{k}_{\parallel} channel.

III. RESULTS AND DISCUSSION

We will demonstrate the effects of various kinds of disorder on the electronic transport in Co|Cu|Co-based trilayers connected to ideal semi-infinite Cu leads, namely, the effects of the interdiffusion at interfaces and of alloying in the spacer. In all cases we consider the fcc(001) structure and the CPP geometry. The equilibrium lattice constant of Cu ($a = 3.55 \text{ \AA}$) is assumed.

A. Numerical implementation

In principle, one should use the potential parameters determined self-consistently for each configuration of the system. Because this approach is numerically prohibitive, we have used self-consistent CPA potential parameters determined for a given alloy composition.³ The same parameters were employed for various random configurations (for more details see Ref. 4). We have thus neglected all fluctuations of the potential parameters due to the variation of the local environment as well as their layer dependence and assumed that the potential parameters take only two values (one common for all A atoms and the other value common for all B atoms).

Layerwise substitutional alloys $A_{1-x}B_x$ are simulated by randomly occupying a chosen (in-plane) supercell with A and B atoms, such that their ratio corresponds to the overall concentration x assumed for a given layer. The random con-

figurations were generated using the RM48 random number generator.⁷ We have used 5×5 supercells corresponding to a $A_{84}B_{16}$ random substitutional alloy, namely, 21 A atoms and four B atoms. The conductances were usually averaged over six configurations and the results agreed within 1–3% with each other.

The \mathbf{k}_{\parallel} integration covers 10 000 points in the full fcc(001) SBZ and 400 points in the 5×5 SCSBZ. In all cases we have employed $|\text{Im} z_{\pm}| = 10^{-7} \text{ Ry}$, where $z_{\pm} = E \pm i\delta$ is a complex energy. The diffusive conductances are calculated as $C_{\text{diff}} = C - C_{\text{ball}}$, $C_{\text{diff}}^{\sigma} = C^{\sigma} - C_{\text{ball}}^{\sigma}$.

B. Ideal trilayer

As a reference system we consider the ideal trilayer $|5 \text{ Co}|s \text{ Cu}|5 \text{ Co}|$ with varying spacer thickness s connected to ideal semi-infinite Cu leads. The electron transport is collisionless with the exception of the slab boundaries, where the electron waves are partially reflected. \mathbf{k}_{\parallel} is conserved, so the transport is solely ballistic and the diffusive transport is missing. The quantum-size effects cause the oscillations of partial resistances, which in turn lead to the oscillations of the GMR ratio R_{CPP} around a value of about 115% (see Ref. 4). The amplitudes are damped with increasing spacer thickness roughly as s^{-1} (see also Ref. 8).

C. Effects of disorder

In the present case, disorder can cause the following effects: (i) an increase of the overall amount of scattering that in turn contributes to a reduction of the transmission probability; (ii) a violation of the strict conservation of the \mathbf{k}_{\parallel} vector belonging to the SBZ of leads can open new transmission channels that contribute to an increase of the conductance; and (iii) interdiffusion smoothens the potential barriers in the ideal trilayer, which in turn also leads to an increased transmission coefficient. Therefore, the net influence of disorder on the conductance results from a competition between all these effects and may lead to an increase or decrease of the conductance, depending on the system under consideration (see also Ref. 9).

D. Interface interdiffusion

We have considered a simple model of the interface interdiffusion for the trilayer $\dots \text{Cu}|5 \text{ Co}|s \text{ Cu}|5 \text{ Co}| \text{Cu} \dots$ in which the interdiffused region extends over two neighboring layers of compositions $\text{Co}_{84}\text{Cu}_{16}$ (on the Co side) and $\text{Co}_{16}\text{Cu}_{84}$ (on the Cu side) at each interface. The resistances change very little with the varying spacer thickness because the number of disordered layers remains constant and possible quantum oscillations are damped by the disorder. The average values of conductances and resistances are given in Table I. In comparison with the ideal trilayer the GMR ratio R_{CPP} is reduced considerably (approximately to 40%). This result is opposite to that of Butler *et al.*¹⁰ and of Zahn *et al.*,¹¹ who found a large increase of the GMR with interface interdiffusion. In contrast to our calculations that assume a ballistic regime for periodically repeated lateral supercells, these authors considered a diffusive regime of conduction,

TABLE I. Spin-resolved average conductances per one surface atom (in units e^2/h) and the GMR ratio R_{CPP} calculated for an fcc (001) $\dots \text{Cu}|5 \text{ Co}|s \text{ Cu}|5 \text{ Co}|\text{Cu} \dots$ trilayer with interface interdiffusion. The subscripts P and AP denote the parallel and the antiparallel orientation of the magnetization of the magnetic slabs, respectively. The spin-averaged values are tabulated for antiparallel orientation. The results for ideal system without interdiffusion are given for comparison.

Case	C_{P}^{\uparrow}	$C_{\text{P}}^{\downarrow}$	$\langle C_{\text{AP}} \rangle$	R_{CPP}
CPA	0.7074	0.0149	0.0540	5.694
Ballistic	0.7066	0.0253	0.0682	4.368
Diffusive	0.0259	0.2305	0.2859	-0.552
Total	0.7325	0.2558	0.3541	0.396
Ideal	0.7426	0.2379	0.2276	1.154

both of them use a linearized-Boltzmann-equation-type approach. Butler *et al.*¹⁰ calculated resistivities within the CPA neglecting vertex corrections; Zahn *et al.*¹¹ introduced an additional damping in the relaxation time. Such an approach neglects the diffusive part of conductances, which is large for parallel minority and antiparallel channels leading thus to a strong decrease in $C_{\text{P}}^{\downarrow}$ and $\langle C_{\text{AP}} \rangle$, which in turn gives large values of the GMR ratio R_{CPP} . This is confirmed by our calculations of the CPA and ballistic conductances (see Table I).

E. Alloying in the spacer

The effect of alloying in the nonmagnetic spacer ($\text{Cu}_{84}\text{Ni}_{16}$) on the transport properties of multilayers is shown in Fig. 1 for the system $\dots \text{Cu}|5 \text{ Co}|\text{Cu}_{84}\text{Ni}_{16}|5 \text{ Co}|\text{Cu} \dots$

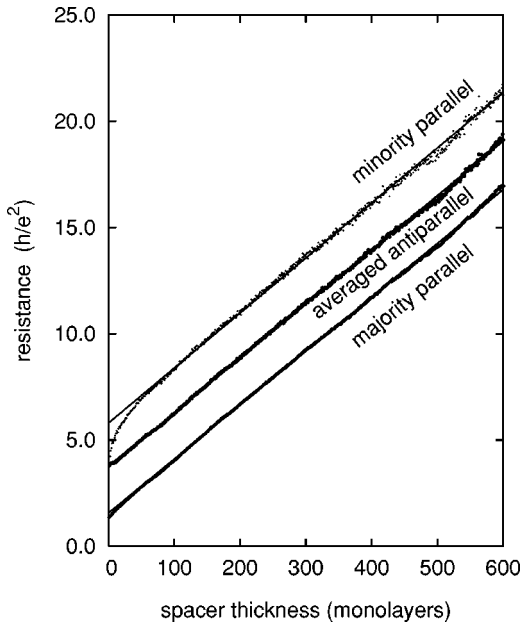


FIG. 1. Partial resistances per one surface atom (in units h/e^2) of an fcc (001) $|5 \text{ Co}|s (\text{Cu}_{84}\text{Ni}_{16})|5 \text{ Co}|$ trilayer embedded between two Cu leads with parallel and antiparallel orientation of the magnetization as a function of the spacer thickness s .

TABLE II. The coefficients A , B , C (in units h/e^2) and D (dimensionless) of the fit (13) of the resistances for the $|5 \text{ Co}|s (\text{Cu}_{84}\text{Ni}_{16})|5 \text{ Co}|$ trilayer with randomness in the spacer embedded between two Cu leads and for $|s (\text{Cu}_{84}\text{Ni}_{16})|$ embedded between two Co leads.

Channel	A	B	C	D
$\dots \text{Cu} 5 \text{ Co} s (\text{Cu}_{84}\text{Ni}_{16}) 5 \text{ Co} \text{Cu} \dots$				
Majority parallel	0.02537	1.5696	-0.2122	0.02643
Minority parallel	0.02589	5.8046	-1.7530	0.05617
Averaged antiparallel	0.02555	3.7309	0.1706	0.42589
$\dots \text{Co} s (\text{Cu}_{84}\text{Ni}_{16}) \text{Co} \dots$				
Majority parallel	0.02517	1.6802	-0.3138	0.01274
Minority parallel	0.02601	2.7742	-1.9806	0.26321
Averaged antiparallel	0.02515	2.4000	-0.2222	0.00564

$\text{Co}|\text{Cu} \dots$. If we neglect small fluctuations due to quantum-size effects, the resistances as functions of the spacer thickness s (measured in monolayers, $1 \leq s \leq 600$) can be, with a good accuracy, expressed by the function

$$\mathcal{R}(s) = As + B + C \exp(-Ds). \quad (13)$$

The coefficients A , B , C , and D were found by a nonlinear least-square fit using the Levenberg-Marquardt method¹² and are given in Table II for systems $\dots \text{Cu}|5 \text{ Co}|s (\text{Cu}_{84}\text{Ni}_{16})|5 \text{ Co}|\text{Cu} \dots$ and $\dots \text{Co}|s (\text{Cu}_{84}\text{Ni}_{16})|\text{Co} \dots$.

The linear increase of resistance with the spacer thickness s is expected in this case because the number of disordered layers increases with the spacer thickness in contrast to the case of interface interdiffusion. The residual bulk resistivity

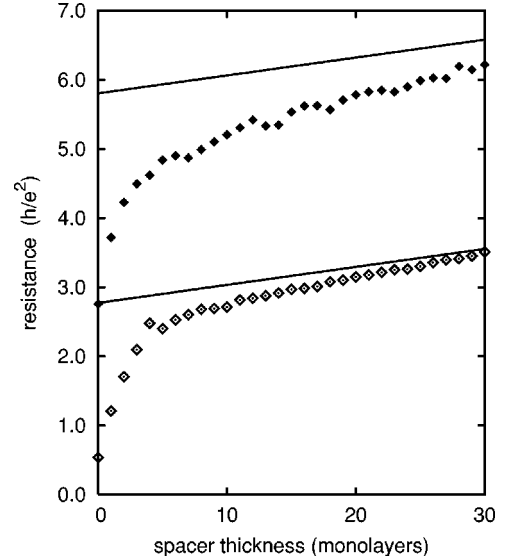


FIG. 2. Resistances per one surface atom (in units h/e^2) of the fcc (001) $|5 \text{ Co}|s (\text{Cu}_{84}\text{Ni}_{16})|5 \text{ Co}|$ trilayer embedded between two Cu leads (filled diamonds) and of a $\text{Cu}_{84}\text{Ni}_{16}$ alloy embedded between two Co leads (empty diamonds) for the parallel orientation of the magnetization as a function of the spacer thickness $0 \leq s \leq 30$. The straight lines show the linear part of the resistance.

TABLE III. Resistances (in units of $\text{f}\Omega \text{m}^2$) of simple systems with at most one magnetic layer.

System	\mathcal{R}_\uparrow	\mathcal{R}_\downarrow	Remark
Infinite Cu	1.73183	1.73183	Sharvin resistance
Infinite Co \uparrow	2.07466	0.87373	Sharvin resistance
... Co \uparrow Cu ...	2.19313	3.26932	Single interface
... Cu 10 Co \uparrow Cu ...	2.19725	4.48903	Two interfaces
... Cu 50 Co \uparrow Cu ...	2.20803	4.93551	Two interfaces

ρ of the alloy forming the spacer is directly connected with the coefficient A by the relation $\rho = AS/d$, where S is the area per one atom in the atomic layer and d is the interlayer distance. Our calculations for both systems give $\rho = 11.8 \times 10^{-8} \Omega \text{m}$, which is somewhat smaller than the experimental value¹³ $\rho_{\text{exp}} = 17.8 \times 10^{-8} \Omega \text{m}$, but it is close to the theoretical value $\rho_{\text{th}} = 10.4 \times 10^{-8} \Omega \text{m}$ obtained by the relativistic KKR-CPA calculations including the vertex corrections¹⁴ for the alloy composition $\text{Cu}_{80}\text{Ni}_{20}$.

The deviations from the linear dependence are observed for smaller spacer thicknesses ($s < 50$); they are particularly large for minority spin electrons and parallel alignment of magnetizations (see Fig. 1 and particularly Fig. 2). This effect is connected with quantum-well states.¹⁵ The resistivity of the alloy in a thin spacer is high, because the quantum-well states are localized and do not contribute to conduction. With increasing spacer thickness the quantum-well states delocalize due to electron scattering into other \mathbf{k}_\parallel states and begin to contribute to electron transport. The resistivity [i.e., the slope of $\mathcal{R}(s)$] decreases and finally it attains its bulk value. The characteristic length of this transition is the electron mean free path. Our results shown in Fig. 1 are similar to those of Tsymbal¹⁶ in his Fig. 2. The main differences, namely, that we do not find nonlinearity in the averaged antiparallel resistance, but observe a large nonlinearity in minority parallel channel can probably be explained by the fact that we assume no disorder in Co layers.

Extrapolation of the linear part of the resistance (13) to zero spacer thickness ($s = 0$), i.e., the constant term B in Eq. (13) yields the total resistance of all interfaces and leads (Sharvin resistance). It is interesting to compare these values with the results found for simple ideal systems such as infinite leads, single interfaces, and trilayers ... Cu| s Co|Cu ... and ... Co| s Cu|Co ... (Table III) as well as with resistances calculated for the ‘‘extrapolated’’ systems ... Cu|10Co|Cu ... and infinite Co (Table IV). No simple relation between these values can be found because the transport in all ideal systems is purely ballistic, and, consequently,

the Sharvin and interface resistances are not additive quantities. The values of the Sharvin resistances of Co and Cu (Table III) agree well with the values reported by Schep *et al.*,¹⁷ the interface resistances $\mathcal{R}_\uparrow = 0.29 \text{ f}\Omega \text{m}^2$ and $\mathcal{R}_\downarrow = 1.97 \text{ f}\Omega \text{m}^2$ agree well with $\mathcal{R}_\uparrow = 0.33 \text{ f}\Omega \text{m}^2$ and $\mathcal{R}_\downarrow = 1.79 \text{ f}\Omega \text{m}^2$ reported by Xia *et al.*¹⁸ for a stronger interdiffusion.

We have calculated separately the ballistic and diffusive conductances for the system ... Cu|5 Co| s ($\text{Cu}_{84}\text{Ni}_{16}$)|5 Co|Cu ... for spacer thicknesses $1 \leq s \leq 150$ and for comparison also the conductance within the CPA. The results are shown in Fig. 3. The ballistic and CPA conductances decrease exponentially with the number s of disordered spacer layers, which corresponds to the loss of charge carriers. A closer examination shows that the ballistic and CPA conductances can be expressed as a sum of several exponential functions and a constant

$$\mathcal{C}(s) = A_0 + \sum_{i=1}^K A_i \exp(-B_i s), \quad (14)$$

where the coefficients A_i and B_i can be found by the same method as before and are given in Table V. It turns out that $K = 3$ is sufficient to obtain a high-quality fit in the sense of the rms error, as can be seen in Fig. 3, where lines corresponding to Eq. (14) fit very closely the calculated points. The constant $A_0 = 0$ for conductances calculated within the CPA, while $A_0 > 0$ for conductances calculated using finite supercells. This indicates a certain limitation of the supercell method. The electron in state \mathbf{k}_\parallel can be scattered into a quasicontinuum of \mathbf{k}'_\parallel states in the real system and the probability that it is later on scattered back into state \mathbf{k}_\parallel is vanishingly small. On the other hand, for finite supercells, the quasicontinuum is replaced by a finite set of \mathbf{k}'_\parallel that after many scattering events (when the distance traveled is larger than the mean free path) will be equally populated. Consequently, even in the limit of an infinite spacer thickness, the ballistic conductance will remain finite and will tend to A_0 . One can expect that $A_0 \propto M^{-1}$, where M is the number of atoms in a supercell. The role of the finite size of supercells and the asymptotic behavior of ballistic and diffusive transport for large thicknesses of the spacer are discussed in the Appendix. The inaccuracy caused by a finite size of supercells becomes noticeable for large spacer thicknesses. A rough estimate follows from an inequality $A_0 > A_1 \exp(-B_1 s)$ that yields 383 \AA (236 \AA) for parallel (antiparallel) magnetization.

The decomposition (14) means that there exist several modes of electron propagation through the disordered spacer with different damping constants. The wave packet that was originally formed in the ideal lead and in the ideal magnetic

TABLE IV. Resistances (in units of $\text{f}\Omega \text{m}^2$) of systems with two magnetic slabs.

System	$\mathcal{R}_\uparrow^{\text{P}}$	$\mathcal{R}_\downarrow^{\text{P}}$	\mathcal{R}^{AP}	Remark
... Co 50 Cu Co ...	2.20475	3.90879	4.16381	
... Co s ($\text{Cu}_{84}\text{Ni}_{16}$) Co ...	2.73286	4.51228	3.91992	Linear extrapolation
... Cu 5 Co 150 Cu 5 Co Cu ...	2.19024	6.93171	7.14632	Ideal system
... Cu 5 Co s ($\text{Cu}_{84}\text{Ni}_{16}$) 5 Co Cu ...	2.58949	9.44333	6.06081	Linear extrapolation

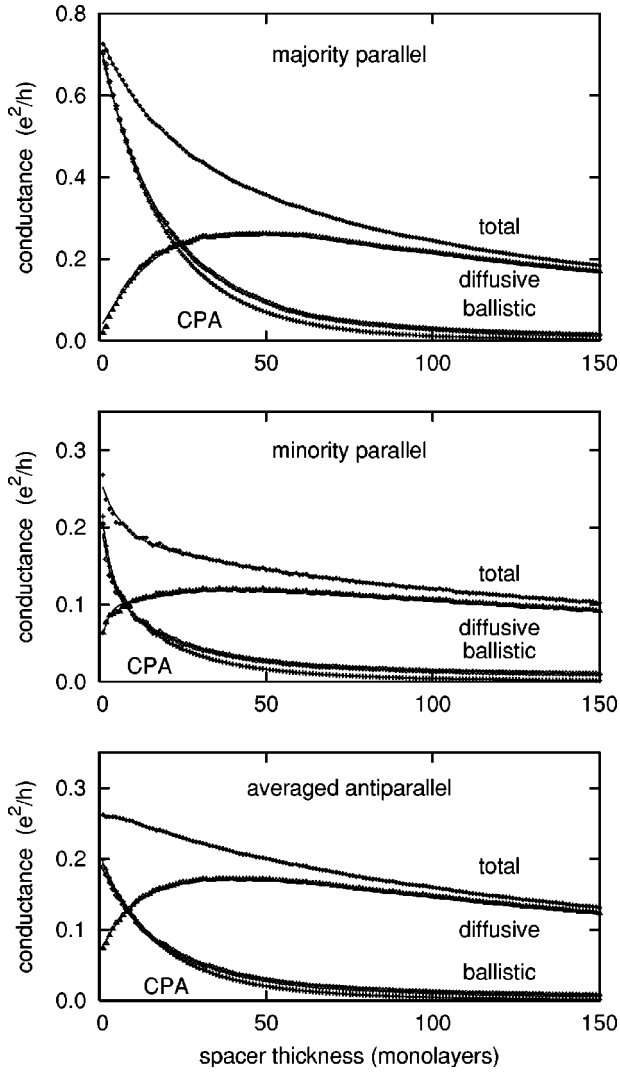


FIG. 3. Partial conductances per one surface atom (in units e^2/h) of an fcc (001) $|5 \text{ Co}|s(\text{Cu}_{84}\text{Ni}_{16})|5 \text{ Co}|$ trilayer embedded between two Cu leads as functions of the spacer thickness s . The total conductance (filled diamonds), its ballistic (empty diamonds) and diffusive (triangles) parts, and the CPA results (+) are shown for the parallel (majority and minority spin) and the antiparallel (spin averaged) alignment of the magnetization.

layer moves into the disordered spacer. Each electron wave in the packet is scattered by the disorder in the spacer with its own scattering rate. Finally a new wave packet with a minimum scattering rate is formed, whose mean free path is given by $\lambda_{\min} = d/B_{\min}$, where B_{\min} is the smallest B_i . We find λ_{\min} for $\dots \text{Cu}|5 \text{ Co}|\text{Cu}_{84}\text{Ni}_{16}|5 \text{ Co}|\text{Cu} \dots$ in the range 103–120 Å from the CPA calculations.

On the other hand, the electron mean free path in a disordered diluted alloy can be roughly estimated from its residual resistivity,¹⁹

$$\lambda = \frac{12\pi^2}{S_F} \frac{h}{e^2} \frac{1}{\rho}, \quad (15)$$

where S_F is the total area of the Fermi surface. Let us assume for simplicity a spherical shape of the Fermi surface and reduction of its radius k_F by alloying Cu with Ni ($\text{Cu}_x\text{Ni}_{1-x}$ alloy), then $S_F = 4\pi k_F^2 = 4\pi(12\pi^2 x)^{2/3} a^{-2}$. This yields $\lambda = 80$ Å for $\text{Cu}_{84}\text{Ni}_{16}$, if the experimental value $\rho_{\text{exp}} = 17.8 \times 10^{-8} \Omega \text{ m}$ is inserted into Eq. (15), while the calculated value $\rho = 11.8 \times 10^{-8} \Omega \text{ m}$ yields $\lambda = 121$ Å in a good agreement with the value of the mean free path derived from our CPA calculations. The calculations based on supercells of finite size yield an anisotropic mean free path because the system is periodic with respect to translations parallel to atomic planes leading thus to infinite mean free path along the atomic planes. This can explain why the resistances obtained from our calculations are somewhat lower than the experimental value. The Sharvin resistance along the atomic planes remains nevertheless finite.

Our results show that the CPA without vertex corrections yields the ballistic part of conductance with a good accuracy, but gives zero for the diffusive conductance as was already discussed in the end of Sec. II D. The diffusive part can only be restored by correctly including vertex corrections, proving their importance in CPA studies of CPP transport in terms of Kubo-Landauer-type approach.⁴

The series-resistor model, elaborated mainly by Lee *et al.*,²⁰ is widely used to interpret experimental data. There is accumulating evidence that it is valid only for diffusive conduction. Butler *et al.*²¹ solved the Boltzmann equation for an interface and have found exponential terms in the electrochemical potential in the vicinity of interface whose charac-

TABLE V. The parameters A_0 , and A_i, B_i , $i=1-3$ of the exponential fit (14) of ballistic and CPA conductances for the $|5 \text{ Co}|s(\text{Cu}_{84}\text{Ni}_{16})|5 \text{ Co}|$ trilayer with randomness in spacer embedded between two Cu leads. The parameters A_i are in units e^2/h , while B_i are dimensionless.

	A_0	A_1	B_1	A_2	B_2	A_3	B_3
	Ballistic						
Parallel	0.008 05	0.030 49	0.006 23	0.251 15	0.026 66	0.597 55	0.064 96
Antiparallel	0.007 32	0.020 28	0.007 65	0.124 66	0.028 04	0.234 34	0.070 48
	CPA						
Parallel	0.000 00	0.042 09	0.015 99	0.532 49	0.042 83	0.356 20	0.086 33
Antiparallel	0.000 00	0.030 20	0.014 82	0.193 21	0.043 20	0.187 82	0.076 45

teristic length is comparable to the electron mean free path. By solving linearized Boltzmann equation, Shpiro and Levy²² have shown that the interface resistance depends on the resistance in the adjacent layers. Bozec *et al.*²³ in their experimental study observed large differences between magnetoresistances of magnetic multilayers that differ only by sequence of magnetic layers (separated and interleaved arrangements), although the series-resistor model predicts that resistances are independent of the layer ordering. Tsymbal¹⁶ calculated the CPP GMR in the Co/Cu multilayers using a realistic tight-binding model and found a thickness-dependent interface resistance that depends on the mean free path. As discussed above, our results confirm these findings. In particular, the results in Table III show a non-additive character of the Sharvin and the interface resistances for systems without disorder. The dependence of the resistances on the thickness of disordered spacer is nonlinear (Fig. 1), but for spacer thicknesses exceeding the mean free path a linear dependence is restored in accordance with the series-resistor model.

IV. CONCLUSIONS

We have presented a systematic *ab initio* study of the influence of alloying in the spacer and at interfaces on the CPP transport in magnetic multilayers. The electronic structure is described by the TB-LMTO method and the Landauer-Büttiker-type approach formulated within the framework of surface Green functions applied to laterally periodic supercells is used to evaluate transport properties.

The main conclusions can be summarized as follows:

(i) Disorder connected with interdiffusion at interfaces between ideal magnetic and non-magnetic slabs can diminish the GMR ratio, but otherwise has a relatively weak effect on the CPP transport through magnetic multilayers.

(ii) The two-current series-resistor model, widely used for interpretation of experimental results, is valid only for large spacer thicknesses. Non-negligible deviations appear for thicknesses comparable to the electron mean free path. Particularly large deviations are found for minority electrons in the parallel alignment of the magnetization that in turn are due to the presence of quantum-well states.

(iii) We have calculated separately the ballistic and diffusive parts of the transport. The ballistic conductance decreases exponentially with the thickness of the disordered spacer and it is approximately equal to the conductance obtained within the CPA without vertex corrections. Consequently, within a Landauer-type description of linear response a correct treatment of vertex corrections in the CPA theory of the CPP transport is necessary.

(iv) We have found that our results, particularly the residual resistivity of the disordered alloy forming the spacer as well as the interface resistances, agree well with experimental data and with other calculations. Also, two independent estimates of the carrier mean free path (from the CPA and from the residual resistivity) are consistent.

(v) The finite size of supercells used in the calculations leads to certain inaccuracies, namely, the resistances and al-

loy resistivities are lowered, the electron mean free path is anisotropic, and the ballistic conductance remains finite even for infinite spacer thickness.

ACKNOWLEDGMENTS

Financial support for this work was provided by the Grant Agency of the Academy of Sciences of the Czech Republic (Projects A1010829 and S2041105), the Grant Agency of the Czech Republic (Project 202/00/0122), the Ministry of Education, Youth, and Sports of the Czech Republic (COST P5.30), the Center for Computational Materials Science in Vienna (GZ 45.504), RTN Computational Magnetoelectronics (Contract HPRN-CT-2000-0143) of the European Commission, and the Scientific and Technological Cooperation between Germany and the Czech Republic (Project TSR-013-98).

APPENDIX: SIMPLE MODEL

We wish to illustrate the role of finite size of supercells and the asymptotic behavior of ballistic and diffusive transport for large thicknesses of a disordered spacer using a simple model based on the following assumptions: (i) the electron entering the disordered spacer layer attains one of the M -allowed values of the transverse momentum \mathbf{k}_\parallel , (ii) in each atomic layer of the disordered region, it may be scattered to another channel \mathbf{k}'_\parallel with probability p . We assume, for simplicity, that the probability p is independent of \mathbf{k}_\parallel and \mathbf{k}'_\parallel , and it is identical for all N disordered layers. We denote the probability that the electron has momentum \mathbf{k}_\parallel after moving through n layers by x_n . Note that the probability to find the electron in one of the other $M-1$ channels different from \mathbf{k}_\parallel is $1-x_n$, and, according to (i), $x_0=1$. If no scattering of electrons from other channels back to \mathbf{k}_\parallel is present, we would find $x_n^{(0)}=(1-p)^n$. This result does not depend on the number of channels M . Clearly, $x_n^{(0)}\rightarrow 0$ for $n\rightarrow\infty$. Backscattering makes things more complex and we can derive a recursion formula

$$x_{n+1}=(1-p)x_n+p(1-x_n)/(M-1) \quad (\text{A1})$$

from which it follows that

$$x_n=\frac{1}{M}+\left(1-\frac{Mp}{M-1}\right)^n\frac{M-1}{M}. \quad (\text{A2})$$

As $x_n\rightarrow 1/M$ for $n\rightarrow\infty$, the limiting value is finite for a finite number of channels, which corresponds to a finite conductance found in supercell calculations even for a very thick spacer. The supercell approach becomes exact in the limit of $M\rightarrow\infty$ and then $x_n\rightarrow 0$. Also the difference between the distribution with backscattering and without it, $\delta_n=x_n-x_n^{(0)}\rightarrow 0$ for $M\rightarrow\infty$. We have thus shown that electron backscattering leads to some error for finite supercells, but this error disappears in the limit of infinite supercells.

- ¹M. N. Baibich, J. M. Broto, A. Fert, F. Nguyen Van Dau, F. Petroff, P. Etienne, G. Creuzet, A. Friederich, and J. Chazelas, *Phys. Rev. Lett.* **61**, 2472 (1988); G. Binasch, P. Grünberg, F. Saurenbach, and W. Zinn, *Phys. Rev. B* **39**, 4828 (1989).
- ²W. P. Pratt, Jr., S.-F. Lee, J. M. Slaughter, R. Loloee, P. A. Schroeder, and J. Bass, *Phys. Rev. Lett.* **66**, 3060 (1991).
- ³I. Turek, V. Drchal, J. Kudrnovský, M. Šob, and P. Weinberger, *Electronic Structure of Disordered Alloys, Surfaces and Interfaces* (Kluwer, Boston, 1997).
- ⁴J. Kudrnovský, V. Drchal, C. Blaas, P. Weinberger, I. Turek, and P. Bruno, *Phys. Rev. B* **62**, 15 084 (2000).
- ⁵P. Weinberger, *Philos. Mag. B* **75**, 509 (1997).
- ⁶P. Bruno, H. Itoh, J. Inoue, and S. Nonoyama, *J. Magn. Magn. Mater.* **198-199**, 46 (1999).
- ⁷F. James, *Comput. Phys. Commun.* **60**, 329 (1990).
- ⁸J. Mathon, A. Umerski, and M. Villeret, *Phys. Rev. B* **55**, 14 378 (1997).
- ⁹S. Zhang and P. M. Levy, *Phys. Rev. B* **57**, 5336 (1998).
- ¹⁰W. H. Butler, J. M. MacLaren, and X.-G. Zhang, in *Magnetic Ultrathin Films, Multilayers and Surfaces/Interfaces and Characterization*, edited by B. T. Jonker, S. A. Chambers, R. F. C. Farrow, C. Chappert, R. Clarke, W. J. M. de Jonge, T. Egami, P. Grünberg, K. M. Krishnan, E. E. Marinero, C. Rau, and S. Tsunashima, *Mater. Res. Soc. Symp. Proc. No. 313* (Materials Research Society, Pittsburgh, 1993).
- ¹¹P. Zahn, J. Binder, I. Mertig, R. Zeller, and P. H. Dederichs, *Phys. Rev. Lett.* **80**, 4309 (1998).
- ¹²W. H. Press, S. A. Teukolsky, W.T. Vetterling, and B. P. Flannery, *Numerical Recipes in FORTRAN* (Cambridge University Press, Cambridge, UK, 1992).
- ¹³S. Legvold, D. T. Peterson, P. Burgadt, R. J. Hofer, B. Lundell, and T. A. Vydrostek, *Phys. Rev. B* **9**, 2386 (1974).
- ¹⁴A. Vernes, H. Ebert, and J. Banhart (unpublished).
- ¹⁵E. Yu. Tsymbal and D. G. Pettifor, *Phys. Rev. B* **61**, 506 (2000).
- ¹⁶E. Yu. Tsymbal, *Phys. Rev. B* **62**, R3608 (2000).
- ¹⁷K. M. Schep, P. J. Kelly, and G. E. W. Bauer, *Phys. Rev. B* **57**, 8907 (1998).
- ¹⁸K. Xia, P. J. Kelly, G. E. W. Bauer, I. Turek, J. Kudrnovský, and V. Drchal, *Phys. Rev. B* **63**, 064407 (2001).
- ¹⁹A. B. Pippard, *Rep. Prog. Phys.* **23**, 176 (1960).
- ²⁰S. F. Lee, W. P. Pratt, Jr., R. Loloee, P. A. Schroeder, and J. Bass, *Phys. Rev. B* **46**, 548 (1992).
- ²¹W. H. Butler, X.-G. Zhang, and J. M. MacLaren, *J. Appl. Phys.* **87**, 5173 (2000).
- ²²A. Shpiro and P. M. Levy, *Phys. Rev. B* **63**, 014419 (2001).
- ²³D. Bozec, M. A. Howson, B. J. Hickey, S. Shatz, N. Wiser, E. Yu. Tsymbal, and D. G. Pettifor, *Phys. Rev. Lett.* **85**, 1314 (2000).